Anti-Idiotypic Antibody Mimics Proteolytic Function of Parent Antigen†

Natalia A. Ponomarenko,‡ Dominique Pillet,§ Marjorie Paon,§ Ivan I. Vorobiev,‡ Ivan V. Smirnov,‡,|| Hervé Adenier,§ Bérangère Avalle,§ Alexander V. Kolesnikov,‡ Arina V. Kozyr,‡ Daniel Thomas,§ Alexander G. Gabibov,‡,⊥,# and Alain Friboulet*,§,#

Shemyakin and Ovchinnikov Institute of Bioorganic Chemistry RAS, 16/10, Miklukho-Maklaya str, Moscow, 117997, Russia, Université de Technologie de Compiègne−CNRS, UMR 6022 Génie Enzymatique et Cellulaire, 60205 Compiègne, France, Department of Chemistry, Lomonosov Moscow State University, Vorobievi gory, Moscow, 119899, Russia, and Institute of Gene Biology, Russian Academy of Sciences, Vavilov St. 34/5, Moscow, 119334, Russia

Received July 16, 2007; Revised Manuscript Received October 4, 2007

ABSTRACT: Functional imaging of subtilisin Carlsberg active center by the idiotypic network yielded a catalytic anti-idiotypic antibody with endopeptidase, amidase, and esterase activities. A monoclonal antibody inhibitory to subtilisin (Ab1 5-H4) was employed as the template for guiding the idiotypic network to produce the catalytic anti-idiotypic Ab2 6B8-E12. Proteolytic activity of 6B8-E12 was demonstrated by zymography using self-quenched fluorescein−BSA conjugate and in a coupled assay detecting Ab2-dependent RNase A inactivation. Cleavage of peptide substrates by 6B8-E12 revealed distinct patterns of hydrolysis with high preference for aromatic residues before or after the scissile bond. Catalytic activity of Ab2 was inhibited by phenylmethylsulfonyl fluoride, a mechanism-based inhibitor of serine hydrolases. 5-H4 and 6B8-E12 were cloned, produced in *Escherichia coli* as single-chain variable fragments (scFvs), and purified. Kinetic parameters for amidolytic and esterolytic activities were similar in Ab2 and its scFv derivative. Although the antigen-specific portion of 6B8-E12 possesses no primary structure similarity to subtilisin, it mimics proteolytic and amidolytic functions of the parental antigen, albeit with 4 orders of magnitude slower acceleration rates. The lack of detectable endopeptidase activity of 6B8-E12 scFv raises interesting issues concerning general evolution of catalytic activity. The in silico 3D models of Ab1 and Ab2 revealed strong structural similarity to known anti-protease antibodies and to abzymes, respectively. These results indicate that the idiotypic network is capable, to a significant extent, of reproducing catalytic apparatus of serine proteases and further validate the use of imaging of enzyme active centers by the immune system for induction of abzymes accelerating energy-demanding amide bond hydrolysis.

Development of a strategy for de novo design of proteases capable of recognizing and specifically cleaving sequences of interest in proteins and peptides and potentially suitable to work in vivo is among the most sought and least tractable goals of modern biochemistry and molecular medicine. Targeted removal of extracellular proteins contributing to certain pathology can be of considerable therapeutic benefit (*1*, *2*). Indeed, modern technologies permit generation of an antibody with specificity to virtually any macromolecular template. Apart from its ability to generate binders specific to a target of choice, the antibody repertoire is widely recognized as a source for generation of "antibody enzymes" (abzymes) with different specificities (*3*, *4*). The first evidence that antibodies can catalyze chemical transformations was brought by immunizing mice with transition state analogs (TSA[1]) (*5*, *6*). Progress in this field has led to development of a number of abzymes, mimicking catalysis of biological transformations as well as catalyzing reactions belonging exclusively to the chemical space (*7*).

In parallel, evidence has been accumulated that catalytic antibodies can be generated spontaneously by the immune system, in the absence of rationally designed immunization. Catalytic immunoglobulins have been documented in the serum of healthy individuals (*8*, *9*), as well as in patients with various diseases (*10*−*16*). Catalytic antibodies can also form in response to infusion of large quantities of a homologous protein; in particular, the abzyme cleaving factor VIII forms in patients with hemophilia A in response to infusion of the therapeutic factor VIII (*17*).

Development of the target-specific (or, within the frame of the immunological terms, epitope-specific) proteolytic abzymes using the TSA approach achieved only limited success (*18*). Importantly, the hydrolytic mechanism of amidase antibodies obtained by the TSA approach differs from that of natural proteases (*19*−*21*). On the other hand,

† This work is supported in part by BTEP Grant #37, RFBR #060449727, NATO SfP #982833.

* Corresponding author. Tel: +33 3-4423-4408. Fax: +33 3-4420-3910. E-mail: alain.friboulet@utc.fr.

‡ Shemyakin and Ovchinnikov Institute of Bioorganic Chemistry RAS.

§ Université de Technologie de Compiègne−CNRS.

|| Lomonosov Moscow State University.

⊥ Institute of Gene Biology RAS.

# These authors made an equal contribution to this research.

[1] Abbreviations: CDR, complementarity-determining region; ELISA, enzyme-linked immunosorbent assay; FBSA, fluorescein bovine serum albumin; mAb, monoclonal antibody; MCA, methylcoumarinamide; PMSF, phenylmethylsulfonyl fluoride; RNase, ribonuclease A; scFv, single chain variable fragment; TSA, transition state analog; VH, variable domain of heavy chain; VL, variable domain of light chain.

10.1021/bi7013954 CCC: $37.00 © 2007 American Chemical Society
Published on Web 11/20/2007

disease-associated abzymes are capable of cleaving macromolecular antigens such as proteins (*22*) or nucleic acids (*15*). Of note, natural abzymes cannot be transition state mimics, due to the absence of transition state analogs in the organism stable enough to drive the immune response. Therefore, other mechanisms can be involved in spontaneous formation of antibody proteases. One plausible explanation for the formation of natural abzymes is provided by the concept of the "functional internal image". According to this concept, an abzyme can form as the functional internal image of the enzyme (auto)antigen through the idiotypic network postulated by Niels Jerne (*23*). This concept has been successfully developed into the methodology of artificially guided development of abzymes with esterase (*24*, *25*) and amidase activity (*26*−*28*). In the cited experiments, functional internal images of acetylcholinesterase and β-lactamase were obtained.

In a previous study, we obtained the first evidence of the amidase and protease activity of anti-idiotypic monoclonal antibody (mAb) elicited by immunization of mice with a mAb specific to the active site of subtilisin Carlsberg (*29*). In this report, we further analyzed structure−functional relationships of anti-idiotypic mAb 6B8-E12 mimicking the functional activity of its parental antigen.

MATERIALS AND METHODS

Molecular Cloning of Ab1 and Ab2. Total mRNA from hybridoma cells 6B8-E12 and 5-H4 was isolated using an Oligotex Direct mRNA Kit (Qiagen) according to the manufacturer's protocol. cDNA was synthesized using SuperScript One-Step RT-PCR with Platinum Taq (Invitrogen). Amplification of the immunoglobulin light-chain variable region (VL) was performed using degenerate forward primers **1**−**4** encompassing N-terminal sequences of mouse κ light chains and degenerate reverse primers **5** and **6** for mouse J-fragments. The heavy-chain variable region (VH) was amplified with the set of degenerate forward primers designed on the basis of the heavy-chain leader sequences (see ref 25) and reverse primers **7**−**10** for J-fragments. Blunt-ended PCR products were cloned into *Eco*RV-digested pGEM5Zf(+) (Promega), and selected clones were sequenced. Primers corresponding to the N-termini (**11**, **12**) and J-fragments (**13**, **14**) of light and heavy chains were constructed on the basis of these sequence data.

The VL of 6B8-E12 was amplified with primers **11** and **13** to append 5′-*Nco*I and 3′-*Bgl*II sites, respectively. The VH of 6B8-E12 was amplified with primers **12** and **14** to introduce 5′-*Nco*I and 3′-*Sal*I sites, respectively. A flexible $(Ser\text{-}Gly_4)_3$ linker was constructed using primers **15**−**17**. The linker was ligated together with VL using *Pci*I and *Nco*I restriction sites, respectively. The resulting VL construct was amplified using primers **15** and **13** and ligated with VH using *Xho*I and *Sal*I restriction sites, respectively. Finally, a single-chain variable fragment (scFv) construct was amplified with primers **12** and **13**, digested by *Nco*I and *Not*I, and cloned between *Nco*I and *Not*I sites of pET22N vector. The latter was prepared on the basis of the pET22b(+) backbone and contained the *Nco*I recognition site in the sequence encoding the periplasmatic leader peptide. An additional fragment, encoding sequences of c-myc epitope and His_6-tag, was cloned into the scFv construct between *Bgl*II and *Not*I recognition sites.

The following are the sequences of the primers used in this work:

1, 5′-GA[A,C]A[A,T]TGTG[A,C]T[C,G]AC[A,C]CA-[A,G]TCTCC[A,T]-3′

2, 5′-GA[T,C]AT[T,C][A,C]AGATGAC[A,C]CAG[A,T]-CT[A,C]C[A,C]-3′

3, 5′-CAAATTGTTCTCACCCAGTCTCCA-3′

4, 5′-GAT[A,G]TT[T,G]TGATGAC[T,C]CA[A,G][A,G]-CT[C,G]CA-3′

5, 5′-TTACGTTT[T,G]ATTTCCA[G,A]CTT[G,T]GTCCC-3′

6, 5′-TTACGTTTCAGCTCCAGCTTGGTCCC-3′

7, 5′-TGAGGAGACGGTGACCGTGGT-3′

8, 5′-TGAGGATACGGGAACCGTGGT-3′

9, 5′-TGCAGAGACACTGACCAGACT-3′

10, 5′-TGAGAAGACGGTGACTGAGGT-3′

11, 5′-TCTTCCTCCATGGGACAAATTGTTCTC-CCCCAGTCTCCA-3′

12, 5′-AGAAGGACCATGGCCGAGGTGCAGCTG-GTGGAGTCTGGGGGA-3′

13, 5′-CTTCTTCGCGGCCGCCAGATCTG-CACGTTTCAGCTCCAGC-3′

14, 5′-TCTCCTTGTCGACACGGTGACCGTGGTC-CCTGC-3′

15, 5′-GAGGAAGCTCGAGTGGTGGTGGTGGT-TCTGGTG-3′

16, 5′-ACCACCACCACTTCCACCACCACCAGAAC-CACC-3′

17, 5′-AGAGGAAACATGTGGGATCCACCACCAC-CACTT-3′

Purification of Ab1 and Ab2 mAbs. Antibodies from culture supernatants were precipitated with ammonium sulfate at 50% saturation at 4 °C. After centrifugation for 30 min at 1400*g*, precipitates were dissolved in phosphate-buffered saline, pH 7.4. Protein A affinity chromatography was done with an Affi-Gel Protein-A MAPS II kit (Bio-Rad) using a 2-mL column according to the manufacturer's instructions. IgG antibodies were eluted with MAPS II elution buffer, pH 2.7 (Bio-Rad). Collected samples were immediately neutralized with 1 M Tris-HCl buffer, pH 9.0, and then dialyzed overnight against 5 mM phosphate buffer, pH 8.0.

Antibodies were further purified by FPLC anion exchange chromatography on a MonoQ HR 5/5 column (Amersham Pharmacia Biotech). The column was equilibrated with 5 mM phosphate buffer, pH 8.0, at a flow rate of 1 mL/min. After injection of protein A-purified antibodies, the column was washed with 4 mL of 5 mM phosphate buffer, pH 8.0. Antibodies were eluted by linear gradient of NaCl (0−200 mM NaCl) over 30 min at 1 mL/min. Collected fractions containing mAbs were pooled and dialyzed against the same phosphate buffer. After centrifugal diafiltration using 30 kDa cutoff Microsep cartridges (7000*g*, 45 min), IgG concentration was determined by the bicinchoninic acid assay (BCA, Sigma). Purified antibodies were subjected to 8% SDS−PAGE, and the purity of IgGs was assessed by silver staining. Molecular sieving performed by gel filtration was done on a FPLC Superdex 200 HR 10/30 column (Amersham Pharmacia Biotech). The column was equilibrated with 0.1 M Tris-HCl buffered saline, pH 7.5, and calibrated with protein standards. Samples were applied, and IgG was separated at a flow rate of 0.5 mL/min.

Expression and Purification of scFv Fragments. Expression of recombinant scFv fragments was performed according to the following general scheme: competent *E. coli* cells BL21(DE3) were transformed by a plasmid DNA; transformants were plated onto Petri dishes containing 1% agar supplemented by 2× YT, 50 μg/mL ampicillin, and 2% glucose; and incubated for 12−14 h at 37 °C. A single colony was used to inoculate 1 L of 2× YT medium containing 100 μg/mL ampicillin and 0.1% of glucose. Bacteria were grown at 37 °C with vigorous agitation to $OD_{600} \sim 0.6-1.0$, and scFv production was induced with 0.1 mM of IPTG. Bacteria were grown for 3 h at 30 °C and harvested by centrifugation. The fraction of soluble recombinant proteins was isolated using a standard protocol (pET System Manual). Recombinant protein was purified by IMAC using Co^{2+}-loaded TALON resin according to the manufacturer's protocol. Proteins were eluted by buffer A (50 mM NaH_2PO_4/Na_2HPO_4, 300 mM NaCl, pH 8.0) containing 50 mM EDTA and dialyzed against TBS.

Analysis of Specificity of Interaction of Ab1−Ab2. SPR Experiments. SPR measurements were done with a BIAcore 2000 apparatus (BIAcore). Whole IgG Ab1 5-H4 was immobilized on a dextran-coated chip by first injecting 35 μL of 0.2 M 1-ethyl-3-(3-dimethylaminopropyl)carbodiimide to activate the surface and then 35 μL of Ab1 at 2 μM. The residual carboxylic groups were subsequently blocked by injecting 1 M ethanolamine at pH 8.5. In all cases, the flow rate was 5 μL/min and the buffer used was 10 mM HEPES buffer, pH 7.4, containing 150 mM NaCl, 3.4 mM EDTA, and 0.005% P20 surfactant. 6B8-E12 (50 μL) at concentrations varying from 0.1 to 4 μM in 10 mM Tris-HCl buffer, pH 8.0, was then injected at a flow rate of 10 μL/min. Kinetic data were analyzed with BIAevaluation software. Prior to analysis of Ab1−Ab2 binding, the readouts were obtained by separately subtracting the control curve obtained with the control surface, activated and deactivated in the absence of Ab1, and the blank curve obtained by running buffer alone on an immobilized surface. Experimental and control curves were obtained simultaneously in parallel using two independent flow systems. Steady state and bivalent analyte models were used for data analysis.

Catalytic Activity Measurements. The amidase activity of subtilisin Carlsberg (EC 3.4.21.62, Sigma) and of 6B8-E12 was assayed by monitoring cleavage of the chromogenic substrates succinyl-Ala-Ala-Pro-Phe-*p*-nitroanilide (AAPF-pNa) and glutaryl-Gly-Gly-Leu-*p*-nitroanilide (GGLpNa) (Sigma) at 410 nm in 0.1 M Tris-HCl, pH 8.6. Substrates were incubated alone under the same conditions, and scored values of spontaneous hydrolysis were subtracted. All experiments were done in triplicate. Kinetic parameters were calculated on the basis of five independent readouts.

Angiotensin II (Bachem), bradykinin, kinetensin, Leu-enkephalin, and substance P (all from Sigma) were used as substrates to evaluate the peptidase activity of 6B8-E12. The antibody (1.2 μM) was incubated with 1 mM peptide in 10 mM Tris-HCl buffer, pH 8.0, at 20 °C for 96 h, and 10-μL aliquots were taken each 12 h during 96 h and kept frozen. Samples were then gently thawed by mixing with 200 μL of ionizing solution containing 50% (v/v) methanol and 0.5% acetic acid (v/v) in water. The solutions were continuously infused in a Finnigan SSQ mass spectrometer equipped with an ion spray (nebulizer-assisted electrospray) source (Analytica of Brandford) with a medical infusion pump at a flow rate varying from 0.2 to 1 μL/min. To inhibit the antibody-mediated peptide cleavage, phenylmethylsulfonyl fluoride (PMSF, Sigma) was added to the incubation medium (100 μM final concentration) prior to the addition of the peptide substrate.

Study of the cleavage of self-quenched bovine serum albumin (BSA) was done according to the original protocol (*30*) with some modifications (*31*). Self-quenched fluorescein−BSA conjugate (FBSA, 0.16 μM) was incubated with 0.5 μM antibody in 0.1M Tris-HCl buffer, pH 7.5, containing 0.1% NaN_3. Hydrolysis of FBSA was measured by a fluorescence microtiter plate reader ($\lambda_{ex} = 495$ nm, $\lambda_{em} = 525$ nm) for 24, 36, 48, 60, and 72 h. The monoclonal anti-idiotypic IgG 4H7-H3 with amidase activity against AAPF-pNa was used as negative control. Fluorescence intensity is measured in arbitrary units (au) and calculated as the difference between the median fluorescence intensity at the time point "*t*" (F_t) and the median fluorescence intensity at the initial time point (F_0): au $= F_t - F_0$. The fluorescence intensity of 0.16 μM FBSA digested by 10 nM trypsin to completion in the same reaction conditions was 230 au.

The degree of inhibition of FBSA cleavage was analyzed by adding 10 μM PMSF or 1 μM aprotinin to the reaction medium containing 1 μM 6B8-E12 just before addition of the substrate. Inhibition of abzyme-mediated FBSA cleavage by Ab1 5-H4 was analyzed at the same concentration of 6B8-E12 and FBSA in the presence of 0.5−3 μM 5-H4.

Detection of Proteolytic Activity of Antibody Sample by Enzymatic Test. First, a calibrating curve was constructed for RNase A concentrations of 0.01−1 ng/μL (PBS/TA buffer). Hydrolysis of polyC by the RNase was performed for 5 min at 37 °C, and reaction was quenched by adding 50% aqueous solution of trichloroacetic acid (TCA) to the final concentration of 10%. Quenched samples were then flash-frozen in liquid nitrogen and stored at −80 °C until use. Samples were centrifuged and diluted 10-fold with water, and their optical density was measured at 274 nm. The obtained values of optical density were subtracted from values of a control sample, polyC, which was incubated without RNase. For assaying the proteolytic activity, the reaction mixture containing 0.15−1.05 μM antibodies and RNase A in the same buffer was incubated at 37 °C for 14 h. The amount of RNase A is taken so that the quantity of the released soluble material with adsorption at 274 nm was within 70% of the upper limit of the determined linear range provided that the RNase A remains intact. After incubation, the mixture was used for hydrolysis of polyC as described above. The degree of degradation of RNase was determinated as the ratio of concentration of RNase A after reaction with abzyme to intact RNase A in percent.

For zymography experiments, 100 or 200 ng of anti-idiotypic mAb was resolved by 10% SDS−PAGE containing 30 μg/mL of FBSA. The latter was impregnated in the gel during polymerization. After washing in 2.5% Triton X-100 for 20 min, the gel was incubated in the dark at 37 °C for 72 h, in 50 mM Tris-HCl, pH 7.6, containing 10 mM $CaCl_2$ and 0.1% NaN_3. Mouse anti-c-myc antibody 9E10 was used as the negative control. Bovine trypsin (100 pg and 1 ng) was used as the positive control. The fluorescence was visualized using a ChemiImager apparatus (Alpha Innotech) with midrange UV illumination and 540 nm optical filter.

The amidase activity of recombinant scFv of 6B8-E12 was studied using a set of methylcoumarinamide (MCA) peptides. Substrates at 50 μM concentration were incubated with 0.75 μM scFv at 37 °C in the dark in PBS, pH 7.5, supplemented with 0.05% NaN_3. A proteolytically inactive irrelevant scFv selected from a phage display library was used as the negative control. Subtilisin Carlsberg was used as the positive control. The fluorescence readout ($\lambda_{ex} = 360$ nm, $\lambda_{em} = 465$ nm) was collected from microtiter plates at different time points using fluorescence reader (Tecan GeNios) equipped with Magellan software (Tecan). MCA peptides were incubated alone, and scored values obtained for spontaneous hydrolysis were subtracted. Kinetic parameters were analyzed using the integral form of the Michaelis−Menten equation.

Computer-Based Homology Model. Structural models of the variable regions of both 5-H4 and 6B8-E12 antibodies were constructed using antibodies of known structure as templates. The VH and VL fragments were initially modeled independently of each other after sequence alignment with sequences represented in the PDB (http://swissmodel.expasy.org/SM_Blast.html) and using the Swiss model server.

Both chains were then superimposed onto the crystal structure of the variable fragment of the antibody demonstrating highest sequence similarity. The atomic coordinates of the modeled structures were then saved as pdb files. Finally, the models were refined by energy minimization with the program Insight II with the Discover module (Accelrys, Orsay, France). The structure refinements were assessed by tracing Ramachandran ϕ/ψ plots to control the absence of conformationally unrealistic regions in the models.

RESULTS

Structural Properties of Ab1 and Ab2 Antibodies. mAb 5-H4 elicited against subtilisin Carlsberg binds to the active site of the protease (*29*, *32*). BALB/c mice were immunized with Ab1 5-H4, and 40 clones were selected for specific binding to the 5-H4 variable region. Among these clones, IgG 6B8-E12 was found to catalyze hydrolysis of AAPFpNa and GGLpNa chromogenic peptide substrates (*29*). This mAb was therefore chosen for further investigation.

Complementary DNAs coding for variable portions of 5-H4 (Ab1) and 6B8-E12 (Ab2) mAbs were cloned, sequenced, and expressed as soluble scFv constructs in *E. coli*. Primary structures of VH and VL fragments of both antibodies are shown in Figure 1. These were aligned to other antibody sequences from the Protein Data Bank. The VH sequence of Ab1 showed best homology with an antibody directed against HIV-1 surface protein p24 (*33*). The VL sequence of Ab1 displays high similarity with the light chain of F11.2.32, an antibody elicited against HIV-1 protease (*34*) and with the light chain of mAb 2b-2F, a mAb that inhibits the ribonuclease activity of angiogenin by interacting with key catalytic residues (*35*). Light-chain sequences of 5-H4 and 2b-2F differ only by five amino acids: one is located in CDR1, two are located in CDR3, and two are in the framework regions. Light-chain sequences of 5-H4 and F11.2.32 differ also by five amino acids: two are located in CDR1 and the three others are in the framework. An intriguing characteristic of F11.2.32 light chain is the protrusion of CDR1 out of the overall immunoglobulin domain fold. The protruding fingerlike structure was proposed to be involved in binding inside the active site of HIV-1 protease (*34*). The 3D model of 5-H4 scFv (Figure 2A) was built using the Insight II software using two structure models from the Protein Data Bank with the high VH+VL homology, 1dzb (anti-lysozyme scFv 1F9 (*36*) and 1jp5 (scFv fragment of anti-HIV-1 protease mAb 1696) (*37*).

The VH sequence of Ab2 6B8-E12 showed high similarity with Q425, an anti-CD4 monoclonal antibody (*38*), and with VH sequence of 2H1, a polysaccharide-binding antibody to *Cryptococcus neoformans* complexed with a peptide from a phage display library (*39*). The VL sequence of 6B8-E12 has high homology with the VL sequence of ANO2, an anti-dinitrophenyl-spin-label antibody (*40*). The 3D model of scFv 6B8-E12 was built (Figure 2B) analogously to that of Ab1 using 1qok (anti-carcinoembryonic antigen scFv) (*41*) as the structure with higher VH+VL homology.

SPR analysis on BIAcore was performed to evaluate binding between Ab1 5-H4 and Ab2 6B8-E12. Whole IgG 5-H4 molecule was immobilized on a dextran sensor chip, and kinetic constants were obtained in four independent experiments. The average association (k_{on}) and dissociation (k_{off}) rate constants were determined as $k_{on} = (4.10 \pm 0.22) \times 10^3$ $M^{-1}.s^{-1}$ and $k_{off} = (1.92 \pm 0.24) \times 10^{-3}$ s^{-1}. The dissociation constant (K_D) for binding of Ab2 to Ab1 was thus evaluated as $(4.68 \pm 0.84) \times 10^{-7}$ M.

Catalytic Properties of the Anti-Idiotypic mAb. Previous studies showed that mAb 6B8-E12 cleaves model chromogenic peptides as well as self-quenched FBSA, revealing not only amidase but also endopeptidase activity (*29*). Monoclonal antibody secreted by the 6B8-E12 hybridoma clone was purified and subjected to size-exclusion chromatography under denaturing conditions according to the previously developed protocol (*15*). After renaturation, amidase and protease activities were retained in the 150 kDa IgG fraction (data not shown). When mAb 6B8-E12 was affinity captured by the immobilized anti-mouse IgG, the proteolytic activity was removed from the supernatant (data not shown). A zymogram analysis using FBSA as the in-gel probe indicates that the proteolytic activity exhibited by mAb 6B8-E12 preparation belongs to the 150 kDa IgG fraction (Figure 3A). Proteolytic activity was also found when the Fab fragment preparation of 6B8-E12 was tested for catalytic activity (Figure 3B). All these results provide evidence for the 6B8-E12 origin of the detected proteolytic activity and rule out any possible contribution of enzyme contamination.

The esterolytic activity of Ab2 was analyzed using *p*-nitrophenyl acetate as the substrate. The good fit of collected data to Michaelis−Menten kinetics for esterase, amidase, and protease reactions catalyzed by the anti-idiotypic abzyme allowed for calculating kinetic parameters and comparing the obtained values with those determined for subtilisin Carlsberg (Table 1). As for the FBSAhydrolysis, esterase and amidase activities of 6B8-E12 were quantitatively removed from solution by immobilized anti-mouse antibodies (data not shown).

The amidase activity of the Ab2 was studied using chromogenic peptides AAPFpNa and GGLpNa. Compared to subtilisin, the amidase activity of Ab2 is rather low ($k_{cat}^{AAPFpNa} = 11\,000 \pm 1500$ and 1.5 ± 0.2 min^{-1} and $k_{cat}^{GGLpNa} = 432 \pm 63$ and 0.5 ± 0.1 min^{-1}, for subtilisin and anti-idiotypic abzyme, respectively). The same conclusion can be drawn for lower antibody affinity for the

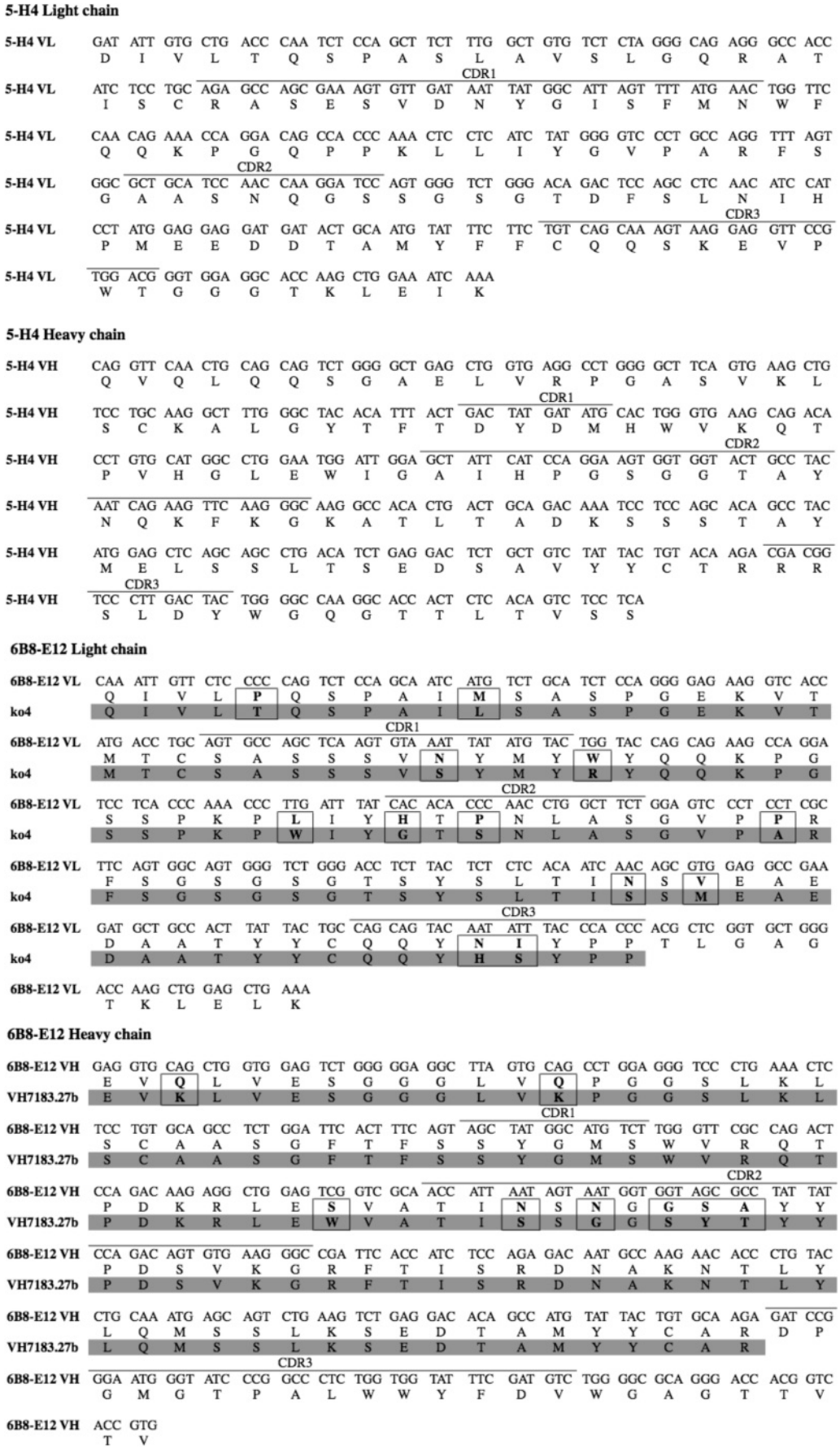

FIGURE 1: Primary structure of variable light and heavy chains of Ab1 5-H4 and Ab2 6B8-E12. The nucleoside sequences of the variable regions of these antibodies have been deposited in the GenBank database and have been assigned accession numbers ef392663 and ef392664 for 5-H4 VH and VL respectively, and ef392665 and ef392666 for 6B8-E12 VH and VL respectively. VL and VH of 6B8-E12 were compared with their equivalent germline (accentuation by gray). Boxes indicate amino acids different from germline.

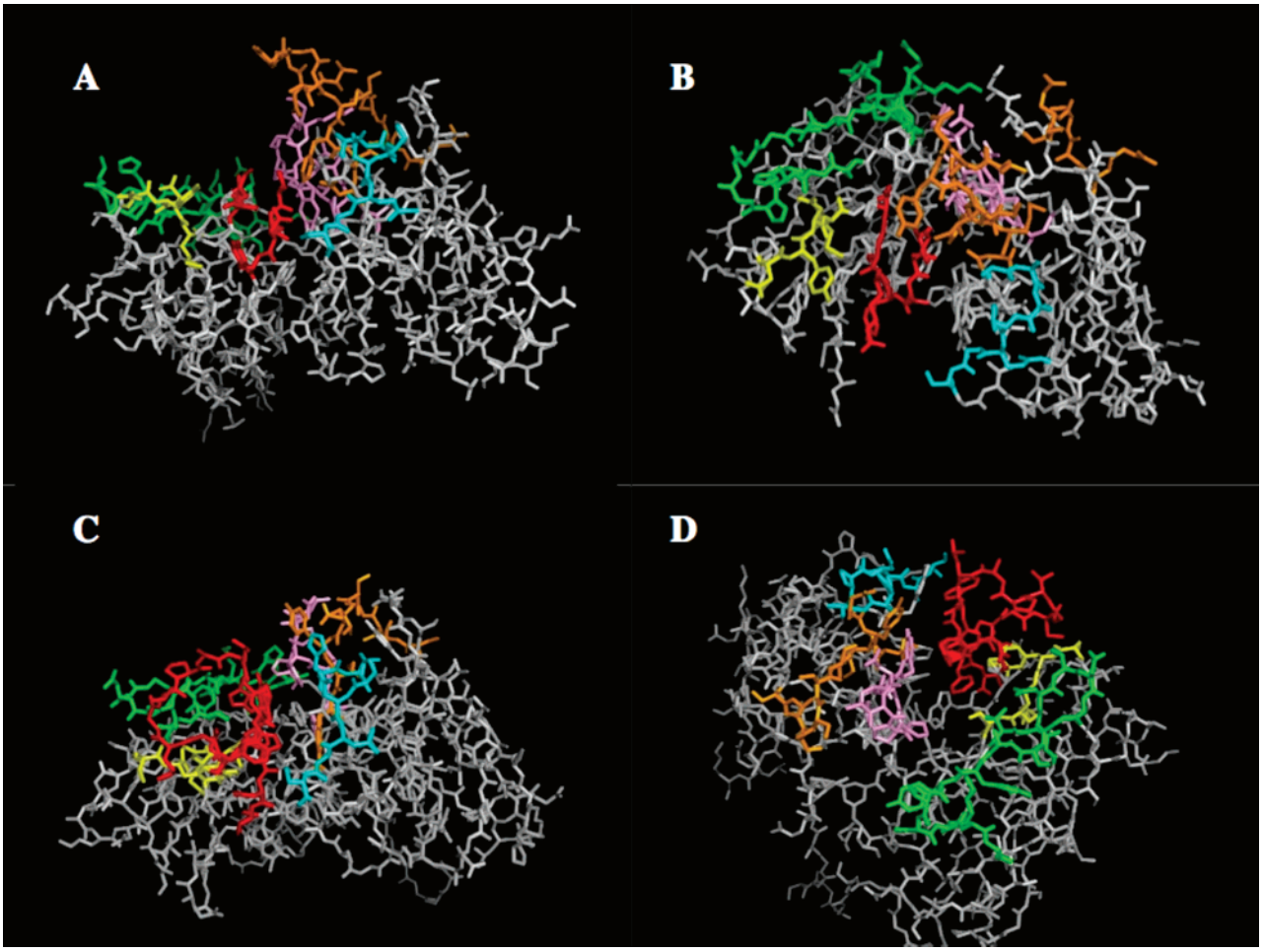

FIGURE 2: Rendered images of the 3-D models of Ab1 5-H4 and Ab2 6B8-E12 scFvs. (A) Side view and a top view of the modeled structure of 5-H4 scFv with the characteristic protruding fingerlike structure formed by VL CDR1 and CDR3. (B) Rendered top view of 5-H4 scFv. (C and D) Side and top views, respectively, for the modeled structure of 6B8-E12 scFv with the typical cleft between VH and VL CDRs. Colors indicate VH CDR1 (yellow), CDR2 (green), and CDR3 (red) and VL CDR1 (orange), CDR2 (cyan), and CDR3 (pink).

substrates when K_m values are compared. Interestingly, when catalytic efficiencies (k_{cat}/K_m) for catalysis of amide substrates are compared, both 6B8-E12 and subtilisin exhibited clear preference for AAPFpNa over GGLpNa. When esterase activities are compared using *p*-nitrophenyl acetate as a substrate, catalytic parameters determined for subtilisin were close to those of 6B8-E12. This could be explained on the one hand by the low efficiency of esterase activity of subtilisin and on the other hand by the fact that the measured activity corresponds to a background hydrolysis by protease catalysts of ester bonds with low activation energy.

In order to further characterize the specificity of peptide bond cleavage by 6B8-E12, nonactivated small bioactive peptides (Leu-enkephalin, Tyr-Gly-Gly-Phe-Leu; angiotensin II, Asp-Arg-Val-Tyr-Ile-His-Pro-Phe; bradykinin, Arg-Pro-Pro-Gly-Phe-Ser-Pro-Phe-Arg; kinetensin, Ile-Ala-Arg-Arg-His-Pro-Tyr-Phe-Leu; and substance P, Arg-Pro-Lys-Pro-Gln-Gln-Phe-Phe-Gly-Leu-Met) were used as substrates to probe the abzyme proteolytic activity. Each peptide taken at 1 mM was incubated with 1.2 μM 6B8-E12 in 10 mM Tris-HCl buffer, pH 8.0, and accumulation of hydrolysis products was detected by ion spray mass spectrometry. Peptides incubated in buffer alone or in the presence of 1.2 μM 5-H4 mAb (Ab1) were taken as the negative control for the cleavage reaction. After the 96-h, incubation, Leu-enkephalin, angiotensin II, bradykinin, and kinetensin, but not substance P, were hydrolyzed by the anti-idiotypic abzyme. No peptide hydrolysis was catalyzed by the 5-H4 mAb. Peptide cleavage sites determined in mass spectrometry experiments are shown in Figure 4. Bradykinin was cleaved only once, whereas several cleavage sites were detected in Leu-enkephalin, angiotensin, and kinetensin. Analysis of cleavage sites reveals certain preferences of the anti-idiotypic abzyme. Preferred scissile bonds are located either before or after hydrophobic residues, preferably aromatic ones, although the Ile-Ala in kinetensin was also cleaved. No scissile bonds were found around charged residues, aliphatic polar residues, or with a proline at P′1. Thus, peptide hydrolysis by Ab2 6B8-E12 exhibits amino acid specificity.

We have previously shown that the protease activity of 6B8-E12 can be revealed by using FBSA and by measuring the decrease of catalytic activity of RNase A induced by the enzyme hydrolysis or by visualizing RNase degradation profiles by SDS gel electrophoresis (*29*). Kinetics of hydrolysis of FBSA can be assayed by absorption/fluorescence spectroscopy techniques (Figure 5A). A lag phase occurring before the catalytic activity was observed. The lag phase has been previously described for antibodies catalyzing esterase and protease activities (*42*, *43*) and was attributed to slow substrate-induced conformational changes of the catalyst. The catalytic mechanism of the Ab2 was probed by the serine protease inhibitors PMSF and aprotinin, a competitive and

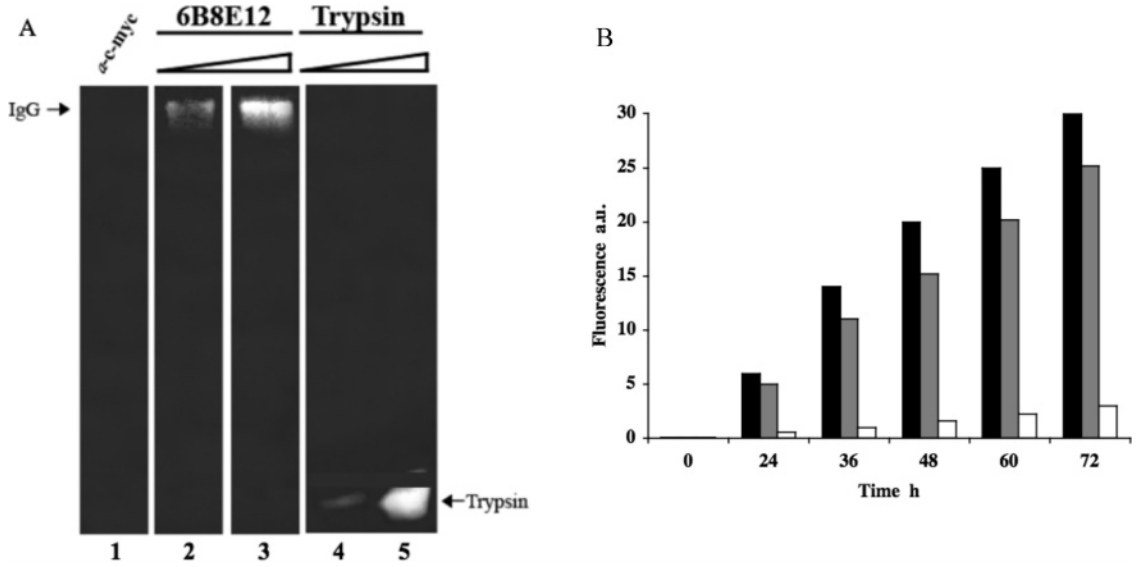

FIGURE 3: Proteolytic activity of 6B8-E12 anti-idiotypic mAb. (A) The anti-idiotypic antibody 6B8-E12 (100 and 200 ng, lanes 2 and 3, respectively) was separated by 10% SDS−PAGE with FBSA impregnated in the gel during polymerization (see Materials and Methods for details). After electrophoresis, proteins were in-gel renatured by Triton X-100 washes. Proteolytic degradation was visualized by the increase in fluorescence intensity, seen as bright bands at the dark background. Mouse anti-c-myc antibody 9E10 was used as the negative control (lane 1). Bovine trypsin (100 pg and 1 ng, lanes 4 and 5, respectively) was used as the positive control. (B) Time course of unquenching of the FBSA fluorescence by the anti-idiotypic abzyme. Concentrations of antibody and F(ab) fragment were 0.5 μM, and substrate was 0.16 μM. Measurements of fluorescence (λ_{ex} = 495 nm; λ_{em} = 525 nm) were done directly on microtiter plates at different times. F(ab) fragment of 6B8-E12 (gray), Ab2 6B8-E12 (black), and amidase IgG 4H7-H3 (white) used as negative control (*29*). Degree of total trypsin digestion of FBSA was 235 fluorescence au (not shown).

Table 1: Comparison of Kinetic Parameters for Amidase and Esterase Activities of Ab2 6B8-E12 and Subtilisin Carlsberg[a]

	subtilisin Carlsberg			6B8-E12		
substrate	k_{cat} (min^{-1})	K_m (mM)	k_{cat}/K_m ($mM^{-1}\,min^{-1}$)	k_{cat} (min^{-1})	K_m (mM)	k_{cat}/K_m ($mM^{-1}\,min^{-1}$)
AAPFpNa	11000 ± 1500	0.20 ± 0.03	55000 ± 16000	1.5 ± 0.2	1.4 ± 0.3	1.1 ± 0.4
GGLpNa	432 ± 63	0.26 ± 0.05	1662 ± 560	0.5 ± 0.1	3.2 ± 0.5	0.2 ± 0.04
p-nitrophenyl acetate	24 ± 5	1.45 ± 0.34	17 ± 7	16.2 ± 3.7	2.6 ± 0.7	6.2 ± 3.1

[a] Amidase activity of subtilisin Carlsberg and of 6B8-E12 (1 μM final concentration) was assayed by monitoring the cleavage of succinyl-Ala-Ala-Pro-Phe-*p*-nitroanilide (AAPF*p*Na) and glutaryl-Gly-Gly-Leu-*p*-nitroanilide (GGL*p*Na) at 410 nm in 0.1 M Tris-HCl, pH 8.6. Esterase activity was estimated by monitoring the hydrolysis of *p*-nitrophenyl acetate by subtilisin Carlsberg and 6B8-E12 (0.46 μM final concentration) at 410 nm in 0.1 M phosphate buffer, pH 7.6. The experiments were performed in triplicate. Kinetic parameters were calculated from five independent measurements.

reversible inhibitor of trypsin-like serine proteases. Cleavage of FBSA by 6B8-E12 was inhibited by Ab1 5-H4 (Figure 5B) and by PMSF, but not by aprotinin (Figure 5A).

Catalysis of Peptide Bond Cleavage by scFv Derivative of the 6B8-E12. Recombinant scFv derived from the Ab2 was expressed and purified and its functional activity was investigated. The scFv retained binding capacity to the Ab1, judging by ELISA (data not shown) and hydrolyzed peptide substrates. However, we failed to show endopeptidase activity of recombinant scFv in FBSA and RNase A assays. The recombinant scFv cleaved Leu-MCA, Phe-MCA, and Met-MCA peptides. So, cleavage preferences of the scFv generally correspond to those of the parental antibody. Kinetic parameters of scFv-mediated cleavage of fluorogenic substrates were determined and are summarized in Table 2.

DISCUSSION

Functional mimicry of the enzyme active center through transfer of the catalytic interface from the inhibitory idiotypic to the catalytic anti-idiotypic antibody has been previously used to elicit esterase (*20*, *21*) and amidase (*22*, *24*) antibodies based on acetylcholinesterase and β-lactamase, respectively, as the enzymic templates. In the present study, subtilisin Carlsberg was exploited as the template to raise 6B8-E12, a monoclonal IgG with protease activity.

The choice of the adequate idiotypic mAb is critical for accurate reproduction of the functional internal image of enzyme via the idiotypic network (*26*). The 5-H4 mAb (Ab1) was previously selected for its efficient inhibition of subtilisin (*29*). When the primary structure of 5-H4 was compared with that of other antibodies, we found that the heavy chain has high homology with an antibody directed against HIV-1 surface protein p24 and, instructively, that the 5-H4 VL region exhibits close homology with VL of F11.2.32, an antibody known to inhibit activity of HIV-1 protease, and with the light chain of mAb 2b-2F, an antibody that inhibits ribonucleolytic activity of angiogenin by interacting with key catalytic residues. The structure of 5-H4 seems to exhibit a planar surface, usually found at the antibody−protein interface, by its heavy chain and to include protruding loops in its light chain able to be accommodated inside the enzyme active site and guide the immune system toward generation of the functional internal image of the parental enzyme.

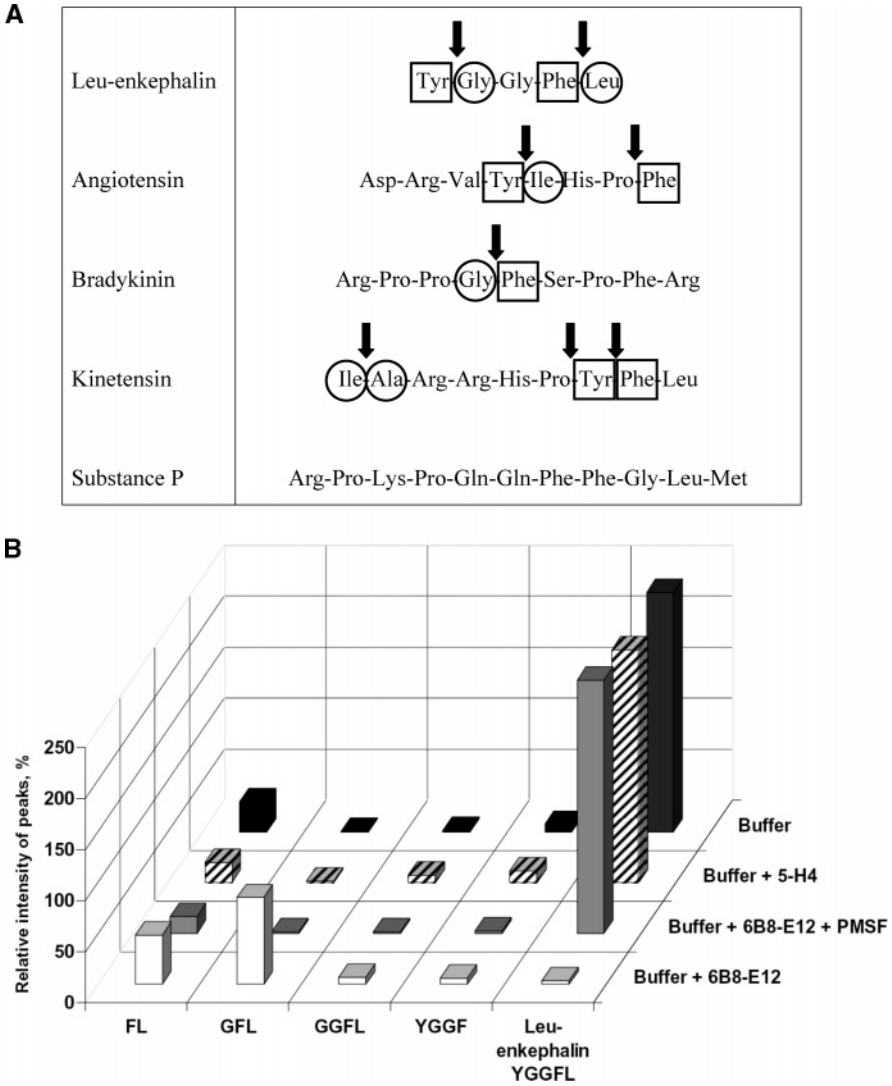

FIGURE 4: Hydrolysis of bioactive peptides by 6B8-E12 monoclonal antibody. (A) Hydrolysis of natural bioactive peptides by anti-idiotypic antibody 6B8-E12 as studied by mass spectrometry. Scissile bonds are marked by arrows; aromatic amino acid residues (squares); aliphatic amino acid residues (circles). (*B*) Leu-enkephalin (1 mM) was incubated in the presence or absence of 6B8-E12 (1.2 μM) in 10 mM Tris-HCl buffer, pH 8.0. The different products of hydrolysis were measured by mass spectrometry after a 96 h incubation period.

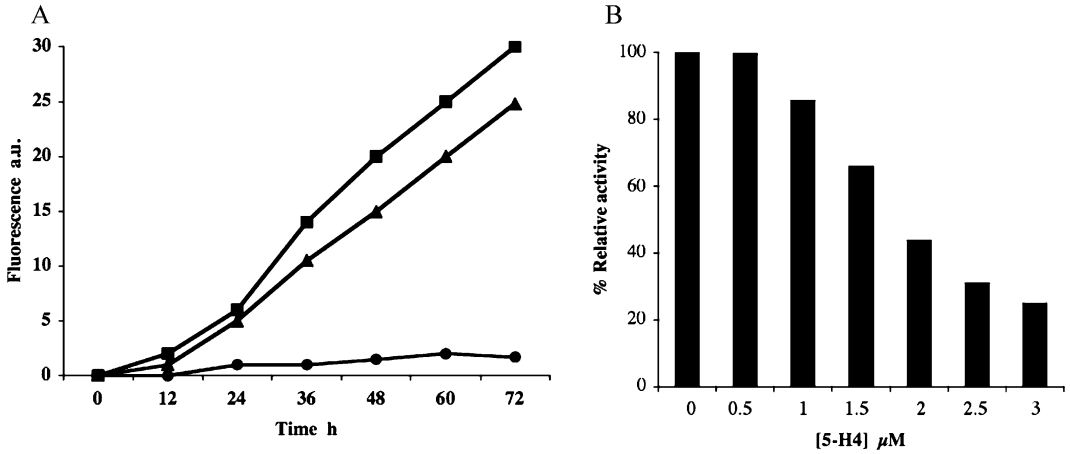

FIGURE 5: (A) Time course of cleavage of FBSA by 6B8-E12. FBSA (0.16 μM) was incubated with 0.5 μM of the abzyme in the absence (■) or presence of 1 μM aprotinin (▲) or 10 μM PMSF (●). (B) Inhibition of FBSA cleavage reaction by the Ab1. The abzyme concentration (6B8-E12) was kept constant at 1 μM, the Ab1 concentration (5-H4) increased from 0 to 3 μM. Relative activity was calculated as a ratio of cleavage rate in the presence of 5-H4 (Vi) to cleavage rate with the abzyme alone (V0) and was expressed in percents (% relative activity).

5-H4 Ab1 was used for eliciting Ab2 by immunizing BALB/c mice. Further screening was done on the basis of the idiotype−anti-idiotype interaction and the ability to hydrolyze chromogenic substrates AAPFpNa and GGLpNa.

Table 2: Kinetic Parameters of Hydrolysis of Model MCA-Amino Acid Substrates by scFv Derivative of 6B8-E12[a]

substrate	k_{cat} (min^{-1})	K_m (mM)	k_{cat}/K_m (mM^{-1} min^{-1})
Met-MCA	0.9 ± 0.2	0.065 ± 0.018	13.9 ± 6.9
Phe-MCA	0.45 ± 0.08	0.009 ± 0.002	52.3 ± 17.0
Leu-MCA	0.52 ± 0.07	0.05 ± 0.01	10.4 ± 3.3

[a] The experiments were performed in triplicate. Kinetic parameters were calculated from five independent measurements.

Screening of the hybridoma panel yielded the 6B8-E12 proteolytic anti-idiotypic antibody (*29*). The primary structure of 6B8-E12 VH showed no significant homology with any element of the primary structure of subtilisin. Within antibody banks, 6B8-E12 VH showed high homology to anti-CD4 mAb Q425 VH and to VH of polysaccharide binding 2H1 mAb. The VL domain of 6B8-E12 exhibits high homology with VL of anti-dinitrophenyl mAb ANO2.

When the 3D model has been prepared, it became evident that the structure of Fv combines the planar characteristics of a typical "protein binder" and a typical "peptide binder", but also with a large cleft between the VH and the VL CDRs with a high concentration of hydrophobic residues. This suggests that hydrophobic substrates might preferentially bind to the antibody combining site. Preliminary data indicated that 6B8-E12 mAb catalyzed hydrolysis of chromogenic peptide substrates with Michaelis−Menten kinetics. Thorough validation of catalytic activity was performed in several distinct ways, such as denaturation−renaturation, repeated purification steps, catalytic activity measurements using antibody fragments, and inclusion of negative controls represented by noncatalytic mAbs. Such a validation procedure allowed us to rule out contamination issues and prove that the activity belongs to the antibody moiety.

Previously, it has been pointed out that it is difficult to find correlates that highlight the fidelity of transfer of the enzyme active center image by the idiotypic network (*25*). Data presented in Table 1 provide some insight in this issue. The k_{cat} value measured for amidase activity of 6B8-E12 is 4 orders of magnitude lower than measured with subtilisin. At the same time, the esterase activity of 6B8-E12 is within the same range as that determined for the enzyme. This could be explained by the fact that subtilisin has been evolved to catalyze hydrolysis of specific peptide bonds with a high-energy barrier, while 6B8-E12 originated as from a structurally altered copy of the enzyme active site. The energy barrier for esterase reaction is significantly lower than for proteolysis, so the structural requirement for expression of such activity can be more relaxed. The esterase activity of both catalysts could represent a certain primitive property exhibited by a catalytic nucleophilic apparatus catalyzing the peptide bond cleavage and not evolved further in subtilisin. It is unlikely that, given the significant difference between the structure of antibody and enzyme, the proteolytic activity of the former can achieve the value comparable to that of the enzyme in a single round. At the same time, a similar level of esterolytic activity in protease and in antibody suggests that the natural evolutionary precursor of subtilisin could possess proteolytic activity comparable to that observed in the antibody. This in turn suggests that, starting from the obtained antibody-based catalytic apparatus, one can achieve the increase in the proteolytic activity using the in vitro evolution. In the present study, we further investigated kinetic parameters and cleavage specificity characteristics of the anti-idiotypic protease. In particular, it was of interest if the antibody cleavage specificity resembles to any extent the cleavage preferences of subtilisin. The specificity of peptide bond cleavage by 6B8-E12 was investigated using several short peptides and the mass spectrometry readout. While only one cleavage site was found in bradykinin, two or even three cleavage sites were detected in Leu-enkephalin, angiotensin, and kinetensin. The substance P peptide was found to not be hydrolyzed by the anti-idiotypic abzyme. Thus, the abzyme does not hydrolyze the peptide bond when a charged residue, either basic or acidic, is present at the P′1 or P1 position. Most of the cleavage sites were found near an aromatic residue, and once between aliphatic residues (Ile-Ala in kinetensin). On the other hand, hydrolysis was never observed when a proline residue is present at position P′1 of a peptide bond or when a residue containing amide in the side chain is present at position P′1 or P1. This specificity of peptide bond cleavage by 6B8-E12, especially for lack of peptide bond hydrolysis near a charged residue, could be related to hydrophobic and aromatic residues populating the antibody combining site. In particular, since the VL domain of 6B8-E12 possesses high homology to the VL of anti-dinitrophenyl-spin-label antibody, this can provide a partial explanation of the antibody cleavage preference to aromatic and hydrophobic amino acid side chains. Although more data on cleavage specificity is needed for detailed description of the Ab2 cleavage specificity, the above observations suggest similarity between cleavage preferences of the catalytic antibody and parental enzyme.

The catalytic efficiency of the Ab2 is comparable with the catalytic efficiency of other peptidase and amidase antibodies (Table 2 and refs *44*−*46*). Interestingly, k_{cat} values of amide bond hydrolysis for the Ab2 are 1−2 orders of magnitude higher than the relevant k_{cat} values of naturally occurring (*46*) and artificial anti-TSA catalytic antibodies (*45*). Relatively high k_{cat} values and the above-described substrate specificity of the Ab2 suggest that combinatorial selection and rational design can be applied to this antibody to generate a protease efficiently cleaving narrow range of hydrophobic substrates.

Endopeptidase activity of Ab2 was also investigated using FBSA as the substrate. An important feature of FBSAhydrolysis is the lag time period observed before the unquenched fluorescence emerged. Similarly, the lag phase was observed when studying other antibodies with esterase and protease activities (*42*, *43*). In these works, the lag-phase phenomenon was explained by slow substrate-induced conformational changes of the catalyst. Such induced conformational changes have been described and clearly demonstrated by comparison of antibodies crystallized in the absence or in the presence of their peptide antigen. The antibody conformational changes described in complex or in the absence of the antigen range from side-chain rearrangements and small segmental movements in the CDR loops to a major rearrangement of the H3 loop in Fab 17/9 (*47*). A conformational change was described for peptide binding by mAb 2H1, the antibody found to have VH high sequence homology with 6B8-E12 heavy domain (*39*). Understanding the actual mechanism underlying the observed

lag phase can help to significantly improve the catalytic efficiency of antibody and its derivatives. Cleavage of peptides and FBSA by 6B8-E12 was inhibited by PMSF, a serine protease inhibitor. This result clearly suggests that a nucleophilic amino acid residue (presumably serine) is critical for catalysis mediated by the anti-idiotypic antibody.

Demonstration of catalytic activity of scFv derived from cDNA of Ab2 was the most compelling evidence that proteolysis occurs due to an intrinsic property of the Ab2 and is not due to contamination issues. The absence of data on activity of recombinant fragments derived from catalytic mAbs often impedes the final proof on existence of specific antibody-dependent catalysis. As was shown, the recombinant scFv of 6B8-E12 is functionally active, judging by the amidase activity and specific binding to Ab1. Recombinant scFv revealed the same substrate specificity with MCA-peptides as subtilisin. Failure to demonstrate the endopeptidase activity of scFv can be due to the inherent difference between thermodynamic properties of the full-length antibody and the artificial assembly of its variable domains. The interaction between heavy and light chain in the antibody is rather stable, whereas it is not always the case for scFv subunits interconnected by a flexible linker. It was noted above that proteolysis of FBSA was preceded by a lag phase presumably needed for the correct superposition of slow-cleaving protease against the scissile bond. It can be speculated that fast changes in the scFv conformation in solution due to its inherent flexibility interfere with the slow movements needed to bind a peptide and overcome the energy barrier of peptide bond hydrolysis. Although scFv fails to cleave peptide bond, it catalyzes less energetically demanding cleavage of terminal amide bonds with good efficiency (Table 2). Methodology of scFv stabilization has been developed (*48*). It will be therefore interesting to investigate whether thermodynamic stabilization of the scFv, in particular, the VH−VL interaction, will result in the increase of the catalytic efficiency. Creation of proteolytic enzymes tailored to cleave a sequence of interest will cause a great impact on fundamental biology and on biomedicine as well. Lessons from studies of anti-idiotypic catalytic antibodies suggest that a wide range of reactions, such as esterolysis, amidolysis, and proteolysis, can be reproduced by the transfer of the functional image of the enzyme's active center to an antibody. Generation of the active image of subtilisin Carlsberg protease showed that the structures needed to overcome the energy demanding barrier of peptide bond hydrolysis can be generated through the idiotypic network. The data presented here permits broadening of the comparative analysis of proteolytic antibodies obtained by different methodologies (*49*) in order to pinpoint common structure−functional peculiarities of antibodies needed to overcome the high-energy barrier of peptide bond hydrolysis.

On the basis of the current state of knowledge, it is not possible to identify the nucleophilic residue of the proteolytic anti-idiotype. Molecular modeling, although helpful for explaining a specificity bias of the proteolytic mAb to large hydrophobic residues in the P1′ position of substrates, does not clarify the layout of the putative active center. It is not surprising, given the difficulty in CDR3 modeling and the absence of the appropriate small and high-affinity ligand for docking into the antibody combining site (*50*).

Earlier, it has been found that a proteolytic VIPase light chain has the germline-encoded protease-like active center (*10*). On the basis of this finding, the hypothesis on the innate antibody catalysis has been advanced (*2*). On the contrary, our data on the active center of the first nucleophilic catalytic antibody with esterase activity, 9A8, indicated the principal role of somatic hypermutation in development of the active center, in particular, the reactive serine residue (*25*). Likewise, somatic hypermutation have been implicated in the formation of the active center of several other catalytic antibodies (*51*−*53*). Comparison between sequences of heavy and light chains of mature 6B8-E12 antibody and corresponding germline genes indicated several mutations that might be directly implicated in formation of the antibody active center (Figure 1). These findings warrant further study of the catalytic mechanism and mode of the functional internal image transfer in the 6B8-E12 mAb.

Although the resulting catalytic turnover of the 6B8-E12 needs to be improved, the fact that the quantum difference between esterolysis and proteolysis can be surmounted in artificially generated antibodies paves the way to creation of efficient proteolytic antibodies with the antigen-tailored specificity.

ACKNOWLEDGMENT

Authors express gratitude to Dr. Anna Mikhailova for assistance in kinetic data processing.

REFERENCES

1. Bamias, G., and Cominelli, F. (2006) Novel strategies to attenuate immune activation in Crohn's disease. *Curr. Opin. Pharmacol. 6*, 401−407.
2. Paul, S., Nishiyama, Y., Planque, S., and Tagushi, H. (2006) Theory of proteolytic antibody occurrence. *Immunol. Lett. 103*, 8−16.
3. Hilvert, D. (2005) Mimicking enzymes with antibodies, In *Artificial Enzymes* (Breslow, R., Ed.) pp 89−109, Wiley-VCH, Weinheim.
4. Gabibov, A. G. (2006) Antibody catalysis: Biochemistry, immunology, pathology. *Immunol. Lett. 103*, 1−2.
5. Tramontano, A., Janda, K. D., and Lerner, R. A. (1986) Catalytic antibodies. *Science 234*, 1566−1570.
6. Pollack, S. J., Jacobs, J. W., and Schultz, P. G. (1986) Selective chemical catalysis by an antibody. *Science 234*, 1570−1573.
7. Hilvert, D. (2000) Critical analysis of antibody catalysis. *Annu. Rev. Biochem. 69*, 751−793.
8. Kalaga, R., Li, L., O'Dell, J. R., and Paul, S. (1995) Unexpected presence of polyreactive catalytic Abs in IgG from unimmunized donors and decreased levels in rheumatoid arthritis. *J. Immunol. 155*, 2695−2702.
9. Planque, S., Bangale, Y., Song, X. T., Karle, S., Tagushi, H., Poindexter, B., Bick, R., Edmundson, A., Nishiyama, Y., and Paul, S. (2004) Ontogeny of proteolytic immunity: IgM serine proteases. *J. Biol. Chem. 279*, 14024−14032.
10. Paul, S., Volle, D. J., Beach, C. M., Johnson, D. R., Powell, M. J., and Massey, R. J. (1989) Catalytic hydrolysis of vasoactive intestinal peptide by human autoantibody. *Science 244*, 1158−1162.
11. Shuster, A. M., Gololobov, G. V., Kvashuk, O. A., Bogomolova, A. E., Smirnov, I. V., and Gabibov, A. G. (1992) DNA hydrolyzing autoantibodies. *Science 256*, 665−667.
12. Gololobov, G. V., Chernova, E. A., Schourouv, D. V., Smirnov, I. V., Kudelina, I. A., and Gabibov, A. G. (1995) Cleavage of supercoiled plasmid DNA by autoantibody Fab fragment: Application of the flow linear dichroism technique. *Proc. Natl. Acad. Sci. U.S.A. 92*, 254−257.
13. Li, L., Paul, S., Tyutyulkova, S., Kazatchkine, M. D., and Kaveri, S. (1995) Catalytic activity of anti-thyroglobulin antibodies. *J. Immunol. 154*, 3328−3332.
14. Lacroix-Desmazes, S., Bayry, J., Kaveri, S., Hayon-Sonsino, D., Thorenoor, N., Charpentier, J., Luyt, C. E., Mira, J. P., Nagaraja,

V., Kazatchkine, M. D., Dhainaut, J. F., and Mallet, V. O. (2005) High levels of catalytic antibodies correlate with favorable outcome in sepsis. *Proc. Natl. Acad. Sci. U.S.A. 102*, 4109−4113.

15. Ponomarenko, N. A., Durova, O. M., Vorobiev, I. I., Belogurov, A. A., Telegin, G. B., Suchkov, S. V., Misikov, V. K., Kiselev, S. L., Lagarkova, M. A., Govorun, V. M., Serebryakova, M. V., Avalle, B., Tornatore, P., Karavanov, A., Morse, H. C., Thomas, D., Friboulet, A., and Gabibov, A. G. (2006) Autoantibodies to myelin basic protein catalyze site-specific degradation of their antigen. *Proc. Natl. Acad. Sci. U.S.A. 103*, 281−286.
16. Ponomarenko, N. A., Durova, O. M., Vorobiev, I. I., Belogurov, A. A., Telegin, G. B., Suchkov, S. V., Misikov, V. K., Morse, H. C., and Gabibov, A. G. (2006) Catalytic activity of autoantibodies toward myelin basic protein correlates with the scores on the multiple sclerosis expanded disability status scale. *Immunol. Lett. 103*, 45−50.
17. Lacroix-Desmazes, S., Moreau, A., Sooryanarayana, Bonnemain, C., Stieltjes, N., Pashov, A., Sultan, Y., Hoebeke, J., Kazatchkine, M. D., and Kaveri, S. V. (1999) Catalytic activity of antibodies against factor VIII in patients with hemophila A. *Nat. Med. 5*, 1044−1047.
18. Blackburn, G. M., and Garçon, A. (2000) Catalytic antibodies, in *Biotechnology vol.8*, (Rehm, H. J., and Reed, G., Eds.) pp 404−490, Wiley VCH, Weinheim.
19. Thayer, M. M., Olender, E. H., Arvai, A. S., Koike, C. K., Canestrelli, I. L., Stewart, J. D., Benkovic, S. J., Getzoff, E. D., and Roberts, V. A. (1999) Structural basis for amide hydrolysis catalyzed by the 43C9 antibody. *J. Mol. Biol. 291*, 329−345.
20. Chong, L. T., Bandyopadhyay, P., Scanlan, T. S., Kuntz, I. D., and Kollman, P. A. (2003) Direct hydroxide attack is a plausible mechanism for amidase antibody 43C9. *J. Comput. Chem. 24*, 1371−1377.
21. Benedetti, F., Berti, F., Brady, K., Colombatti, A., Pauletto, A., Pucillo, C., and Thomas, N. R. (2004) An unprecedented catalytic motif revealed in the model structure of amide hydrolyzing antibody 312d6. *Chembiochem 5*, 129−131.
22. Kim, Y. R., Kim, J. S., Lee, S. H., Lee, W. R., Sohn, J. N., Chung, Y. C., Shim, H. K., Lee, S. C., Kwon, M. H., and Kim, Y. S. (2006) Heavy and light chain variable single domains of an anti-DNA binding antibody hydrolyze both double- and single-stranded DNAs without sequence specificity. *J. Biol. Chem. 281*, 15287−15295.
23. Jerne, N. (1974) Towards a network theory of the immune system. *Ann. Immunol. (Paris) 125c*, 373−389.
24. Izadyar, L., Friboulet, A., Rémy, M. H., Roseto, A., and Thomas, D. (1993) Monoclonal anti-idiotypic antibodies as functional internal images of enzyme active sites: Production of a catalytic antibody with a cholinesterase activity. *Proc. Natl. Acad. Sci. U.S.A. 90*, 8876−8880.
25. Kolesnikov, A. V., Kozyr, A. V., Alexandrova, E. S., Koralewski, F., Demin, A. V., Titov, M. I., Avalle, B., Tramontano, A., Paul, S., Thomas, D., Gabibov, A. G., and Friboulet, A. (2000) Enzyme mimicry by the anti-idiotypic antibody approach. *Proc. Natl. Acad. Sci. U.S.A. 97*, 13526−13531.
26. Avalle, B., Thomas, D., and Friboulet, A. (1998) Functional mimicry: Elicitation of a monoclonal anti-idiotypic antibody hydrolyzing β-lactams. *FASEB J. 12*, 1055−1060.
27. Débat, H., Avalle, B., Chose, O., Sarde, C. O., Friboulet, A., and Thomas, D. (2001) Overpassing an aberrant Vk gene to sequence an anti-idiotypic abzyme with β-lactamase-like activity that could have a linkage with autoimmune diseases. *FASEB J. 15*, 815−822.
28. Padiolleau-Lefèvre, S., Débat, H., Phichith, D., Thomas, D., Friboulet, A., and Avalle, B. (2006) Expression of a functional scFv fragment of an anti-idiotypic antibody with a β-lactam hydrolytic activity. *Immunol. Lett. 103*, 39−44.
29. Pillet, D., Paon, M., Vorobiev, I. I., Gabibov, A. G., Thomas, D., and Friboulet, A. (2002) Idiotypic network mimicry and antibody catalysis: Lessons for the elicitation of efficient anti-idiotypic protease antibodies. *J. Immunol. Methods 269*, 5−12.
30. Voss, E. W., Workmann, C. J., and Mummert, M. E. (1996) Detection of protease activity using a fluorescence-enhancement globular substrate. *Biotechniques 20*, 286−291.
31. Ponomarenko, N. A., Durova, O. M., Vorobiev, I. I., Alexandrova, E. A., Telegin, G. B., Chamborant, O. A., Sidorik, L. L., Suchkov, S. V., Alekberova, Z. S., Gnuchev, N. V., and Gabibov, A. G. (2002) Catalytic antibodies in clinical and experimental pathology: Human and mouse models. *J. Immunol. Methods 269*, 197−211.
32. Avalle, B., Friboulet, A., and Thomas, D. (1998) Screening of inhibitory monoclonal antibody. A critical step for producing anti-idiotypic catalytic antibodies. *Ann. N.Y. Acad. Sci. 864*, 118−130.
33. Keitel, T., Kramer, A., Wessner, H., Scholz, C., Schreider-Mergener, J., and Höhne, W. (1997) Crystallographic analysis of anti-p24 (HIV-1) monoclonal antibody cross-reactivity and polyspecificity. *Cell 91*, 811−820.
34. Lescar, J., Stouracova, R., Riottot, M. M., Chitarra, V., Brynda, J., Fabry, M., Horejsi, M., Sedlacek, J., and Bentley, G. A. (1997) Three-dimensional structure of an Fab-peptide complex: Structural basis of HIV-1 protease inhibition by a monoclonal antibody. *J. Mol. Biol. 267*, 1207−1222.
35. Chavali, G., Papageorgiou, A., Olson, K., Fett, J., Hu, G., Shapiro, R., and Acharya, K. R. (2003) The crystal structure of human angiogenin in complex with an antitumor neutralizing antibody. *Structure 11*, 875−885.
36. Aÿ, J., Keitel, T., Küttner, G., Wessner, H., Scholz, C., Hahn, M., and Höhne, W. (2000) Crystal structure of a phage library-derived single-chain Fv fragment complexed with turkey egg-white lysozyme at 2.0 A resolution. *J. Mol. Biol. 301*, 239−245.
37. Rezacova, P., Lescar, J., Brynda, J., Fabry, M., Horejsi, M., Sedlacek, J., and Bentley, G. A. (2001) Structural basis of HIV-1 and HIV-2 protease inhibition by a monoclonal antibody. *Structure 9*, 887−895.
38. Zhou, T., Hamer, D. H., Hendrickson, W. A., Sattentau, Q. J., and Kwong, P. D. (2005) Interfacial metal and antibody recognition. *Proc. Natl. Acad. Sci. U.S.A. 102*, 14575−14580.
39. Young, A. C. M., Valadon, A. C., Casadevall, A., Scharff, M. D., and Sacchettini, J. C. (1997) The three-dimensional structures of a polysaccharide binding antibody to Cryptococcus neoformans and its complex with a peptide from a phage display library: Implications for the identification of peptide mimotopes. *J. Mol. Biol. 274*, 622−634.
40. Brunger, A. T., Leahy, D. J., Hynes, T. R., and Fox, R. O. (1991) 2.9 A resolution structure of an anti-dinitrophenyl-spin-label monoclonal antibody Fab fragment with bound hapten. *J. Mol. Biol. 221*, 239−256.
41. Boehm, M. K., Corper, A. L., Wan, T., Sohi, M. K., Sutton, B. J., Thornton, J. P., Keep, P. A., Chester, K. A., Begent, R. H., and Perkins, S. J. (2000) Crystal structure of the anti-(carcinoembryonic antigen) single-chain Fv antibody MFE-23 and a model for antigen binding based on intermolecular contacts. *Biochem. J. 346*, 519−528.
42. Lindner, A. B., Eshhar, Z., and Tawfik, D. S. (1999) Conformational changes affect binding and catalysis by ester hydrolysing antibodies. *J. Mol. Biol. 285*, 421−430.
43. Hifumi, E., Hatiuchi, K., Okuda, T., Nichizono, A., Okamura, Y., and Uda, T. (2005) Specific degradation of H. pylori urease by a catalytic antibody light chain. *FEBS J. 272*, 4497−4505.
44. Gao, Q. S., Sun, M., Tyutyulkova, S., Webster, D., Rees, A., Tramontano, A., Massey, R. J., and Paul, S. (1994) Molecular cloning of a proteolytic antibody light chain. *J. Biol. Chem. 269*, 32389−32393.
45. Gibbs, R. A., Posner, B. A., Filpula, D. R., Dodd, S. W., Finkelman, M. A., Lee, T. K., Wroble, M., Whitlow, M., and Benkovic, S. J. (1991) Construction and characterization of a single-chain catalytic antibody. *Proc. Natl. Acad. Sci. U.S.A. 88*, 4001−4004.
46. Paul, S., Li, L., Kalaga, R., Wilkins-Stevens, P., Stevens, F. J., and Solomon, A. (1995) Natural catalytic antibodies: Peptide-hydrolyzing activities of Bence Jones proteins and VL fragment. *J. Biol. Chem. 270*, 15257−15261.
47. Schulze-Gahmen, U., Rini, J. M., and Wilson, I. A. (1993) Detailed analysis of the free and bound conformations of an antibody. X-ray structures of Fab 17/9 and three different Fab−peptide complexes. *J. Mol. Biol. 234*, 1098−1118.
48. Monsellier, E., and Bedouelle, H. (2006) Improving the stability of an antibody variable fragment by a combination of knowledge-based approaches: Validation and mechanisms. *J. Mol. Biol. 362*, 580−593.
49. Ponomarenko, N. A., Vorobiev, I. I., Alexandrova, E. S., Reshetnyak, A. V., Telegin, G. B., Khaidurov, S. V., Avalle, B.,

Karavanov, A., Morse, H. C., Thomas, D., Friboulet, A., and Gabibov, A. G. (2006) Induction of a protein-targeted catalytic response in autoimmune prone mice: Antibody-mediated cleavage of HIV-1 glycoprotein gp120. *Biochemistry 45*, 324−330.

50. Whitelegg, N. R. J., and Rees, A. R. (2000) WAM: An improved algorithm for modeling antibodies on the WEB. *Protein Eng. 13*, 819−824.
51. Yin, J., Mundorff, E. C., Yang, P. L., Wendt, K. U., Hanway, D., Stevens, R. C., and Schultz, P. G. (2001) A comparative analysis of the immunological evolution of antibody 28B4. *Biochemistry 40*, 10764−10773.
52. Yang, P. L., and Schultz, P. G. (1999) Mutational analysis of the affinity maturation of antibody 48G7. *J. Mol. Biol. 294*, 1191−1201.
53. Arkin, M. R., and Wells, J. A. (1998) Probing the importance of second sphere residues in an esterolytic antibody by phage display. *J. Mol. Biol. 284*, 1083−1094.

BI7013954